http://dx.doi.org/10.5935/0103-5053.20150145

J. Braz. Chem. Soc., Vol. 26, No. 8, 1710-1717, 2015.
Printed in Brazil - ©2015 Sociedade Brasileira de Química
0103 - 5053 $6.00+0.00

Article

CuO Nanofibers Immobilized on Paraffin-Impregnated Graphite Electrode and its Application in the Amperometric Detection of Glucose

Ícaro A. Simon,[a] Natália G. Medeiros,[a] Ketlin C. Garcia,[a] Rosane M. D. Soares,[a] Aline T. Rosa[b] and Jacqueline A. Silva[a,]*

[a]*Instituto de Química and* [b]*Centro de Microscopia Eletrônica, Universidade Federal do Rio Grande do Sul, P. O. Box 15003, 91501-970 Porto Alegre-RS, Brazil*

1-D nanostructures are promising materials for development of electrochemical devices offering benefits such as fast electron transfer rates and large surface areas. Copper oxide nanofibers (CuO-NFs) synthesized by electrospinning technique and subsequent thermal treatment, were used to modify paraffin-impregnated graphite electrode (PIGE) for a sensitive non-enzymatic glucose detection. The structure and morphology of CuO-NFs were characterized by scanning electron microscopy and transmission electron microscopy. The electrocatalytic activity towards glucose oxidation was evaluated by cyclic voltammetry and chronoamperometry. The results reveal a wide linear response to glucose ranging from 1.0×10^{-6} to 1.93×10^{-3} mol L^{-1} ($R^2 = 0.9927$). The limit of detection was 0.39×10^{-6} mol L^{-1} (LOD = 3σ/s). The high aspect ratio of the nanofibers arranged in a three-dimensional network structure significantly enhances the electron transfer process. The electrode preparation is simple and rapid execution, and more importantly the graphite rod is relative low-cost and easy to achieve surface renewal for reusability.

Keywords: CuO nanofibers, electrospinning, electrocatalysis, glucose sensor, PIGE electrode

Introduction

Diabetes is a widespread chronic metabolic disease, affecting about 347 million people worldwide. According to the World Health Organization (WHO) this can be the 7th leading cause of death in 2030.[1] Early detection and treatment prevents devastating complications such as heart attack, kidney disease, blindness, erectile dysfunction and persistent infections. Nevertheless, unfortunately, the diagnosis is often delayed until complications appear. Hyperglycemia, the high level of glucose in the blood, is the primary cause of pathological consequences of diabetes. Therefore, regular glucose monitoring is mandatory. For routine analysis, it has been established several methodologies that use different enzymatic assays and perform optical or electrochemical detection.[2-4] Among these, electrochemical sensors with immobilized glucose oxidase have been extensively applied due to its high sensitivity and excellent selectivity.[5,6] Nonetheless, these enzymatic electrodes are still suffering some drawbacks, especially regarding the lack of stability due to the intrinsic nature of the proteins, the difficulty of immobilization and the relative high cost of the enzymes. These disadvantages have stimulated intensive research efforts aimed to the development of sensors without using enzymes. The majority of these non-enzymatic electrochemical glucose sensors employ metals or metal oxides as the working electrode by exploring their electrocatalytic activity towards the glucose oxidation.[7] Since the measurement relies on the current response at these electrode surfaces, the type of catalyst as well as the surface structure are crucial for achieving good performance. Thus, nano-dimensioned materials are frequently designed to enhance the analytical performance of the devices. Different nanostructures, including Pt, Pd, Ni, Cu, NiO, CuO, are reported in the literature as useful electrocatalyst for oxidation of glucose.[8-11] Most of them offer high sensitivity, long-term stability, thermal resistance, simple fabrication method, and cost-effective. However, the research for larger surface areas, higher glucose oxidation kinetics, and better selectivity promote a continuous investigation in the designing of new nanomaterials and strategies for the electrode preparation. Among the electrocatalyst commonly used in the development of glucose sensors, copper oxide shows great prospect due to its excellent electrochemical and catalytic properties, high stability and low production cost.[12] A variety of CuO nanostructures has been synthesized by using different techniques. For example, nanoflowers, nanowires, nanoplatelets, and nanorods, were synthesized

*e-mail: jacqueline.arguello@ufrgs.br

by wet chemical route involving NaOH and Cu^{II}.[13-16] Some of them require a sacrificial precursor or template followed by thermal decomposition. Hydrothermal method and electrochemical techniques have also been applied to prepare different CuO nanostructures.[17,18] On the other hand, nanofiber-like structures were achieved by using an electrospinning process and subsequent calcination by Song and co-workers[19] and Xiao and co-workers.[20] The preparation of the electrodes in both cases followed different approaches. While the CuO nanofibers (CuO-NFs) prepared by Song and co-workers were suspended in suitable solvents by ultrasonication and then casted onto a glassy carbon and indium tin oxide (ITO) electrode surfaces. Xiao and co-workers synthesized the nanofibers directly on the ITO surfaces. The *in situ* electrospun improved the analytical performance and also dispensed the use of nafion solution as entrapment matrix. In this work, a nanofiber precursor solution consisted of $Cu(CH_3COO)_2$ dissolved in polyvinyl alcohol (PVA) was electrospun on a glass slide. The CuO nanofibers obtained after calcination was mechanically transferred to a paraffin-impregnated graphite electrode (PIGE) surface. This process of electrode preparation is simple, straightforward and rapid execution, and more importantly the graphite rod is relative low-cost and easy to achieve surface renewal for reusability. Therefore, it is demonstrated that CuO nanofibers on the PIGEs surface are suitable as a working electrode for glucose electrooxidation with high analytical performance. In addition, 1-D nanostructure networks reveal good electrochemical performance as electrode material development of analytical devices.[21]

Experimental

Chemicals

All reagents used were of analytical grade and used as received without any further purification. These were: polyvinyl alcohol (PVA, mw = 85,000-124,000, Aldrich), ascorbic acid (Aldrich), uric acid (Aldrich), dopamine (Aldrich), copper(II) acetate monohydrate (Merck), ethanol (Proquimios), glucose (Merck), potassium ferrocyanide trihydrate (Merck), and sodium hydroxide (Nuclear). Glucose standard solutions were freshly prepared for each assays using deionized water of resistivity not less than 18.2 MΩ cm (Milli-Q purification system, Millipore).

Synthesis of CuO nanofibers

CuO nanofibers were obtained by following the three steps of typical procedures used for preparing metal oxide nanofibers through electrospinning.[19,22] The first step consisted in the preparation of the precursor solution. 0.50 g of copper(II) acetate was dissolved in an aqueous solution of PVA (10.0 wt.%) under vigorous stirring overnight in order to get a homogeneous viscous gel. Secondly, the as-prepared gel was transferred to a syringe and electrospinning at 15 kV at a distance of 12 cm and a flow rate of 2 mL h^{-1} during 12 min. The electrospun nanofibers were collected on the surface of a glass slide placed on grounded aluminum foil and finally the calcination step took place at 500 °C for 3 h. The heating treatment removed the organic constituents and converted the precursor into CuO.

Apparatus

Thermogravimetric analysis and its derivative form (TGA/DTG) were conducted using a TGA Q500 V6.7 Build 203 instrument. The curves were recorded under N_2 atmosphere at a flow rate of 60 mL min^{-1} with a heating rate of 10 °C min^{-1} from 22 to 700 °C. The surface morphology and its chemical composition were examined using a JEOL JSM-5800 microscope equipped with a Noran energy-dispersive spectrometer (EDS). Transmission electron microscopy (TEM) observations were performed by using a JEOL JEM2010 instrument with an accelerating voltage of 200 kV.

The electrochemical measurements were carried out on a MicroAutolab III potentiostat (EcoChemie, The Netherlands). All experiments were performed using a conventional three-electrode system consisting of a saturated calomel reference electrode (SCE), a platinum wire counter electrode, and the CuO-NFs/PIGE as the working electrode. 0.1 mol L^{-1} NaOH solution was employed as the supporting electrolyte.

Preparation of the CuO-NFs/PIGE electrodes

CuO nanofibers were transferred onto a PIGE (2 mm of diameter) by pressing the electrode surface against the glass slide where the fibers were initially formed. After immobilization, the electrode was cycled between 0 to +0.65 V to get a stabilized response. The modified electrode will be denoted as CuO-NFs/PIGE, hereafter.

Results and Discussion

CuO nanofibers characterization

Thermogravimetric analysis (TGA) provides the information about the decomposition of the as-prepared nanofibers during the heat treatment. Figure 1 shows

the TGA/DGA curves of $Cu(CH_3COO)_2$/PVA composite nanofibers. The weight loss below 100 °C corresponds to the hydrated water molecules. After the dehydration, there are three peaks between 200 and 400 °C, the first one can be attributed to the loss of the acetate anion as gaseous carbon dioxide and water. According to the literature, this event occurs at 222 °C.[23] Thus, the other peaks around 275 and 375 °C can be ascribed to the PVA decomposition. The pyrolysis take place in the regions of 300-325 °C and 400-425 °C, and comprise of chain scission reactions.[24] After that there was not significant change.

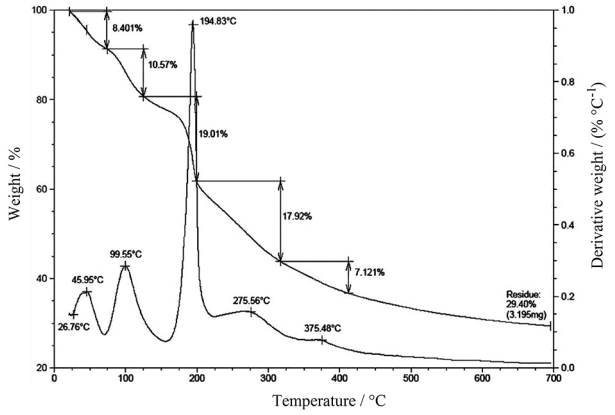

Figure 1. TGA/DTA curves of the as-prepared nanofibers.

Scanning electron microscopy (SEM) images allowed the detailed visualization of the morphologies and sizes of the synthesized CuO nanofibers. It can be seen from Figure 2 that the diameter varies from 100 to 220 nm with micrometer in lengths, resulting in an extremely high aspect ratio. Most of the fibers are touched or fused each other; this interconnection could benefit the electron transfer reaction.

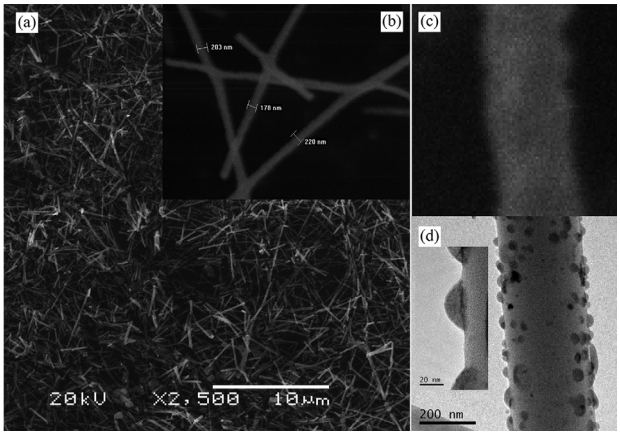

Figure 2. SEM micrographs at magnification of 2,500 times (a) and 40,000 times (b and c) and TEM image (d) of the synthesized CuO nanofibers.

The CuO nanofibers were further characterized by TEM (Figure 2d). The surface of the fibers appears very rough since they seem to consist of an accumulation of CuO nanoparticles. This fact is very interesting because can provide a larger surface area for the catalytic reaction. Figure 3 depicts the EDS spectrum, which helps to confirm the structure of the sample by providing semi-quantitative information about the elemental composition. Only the elements Cu and O are present, and their atomic ratio Cu/O is 1.1, which is approximate to the stoichiometric proportion in CuO.

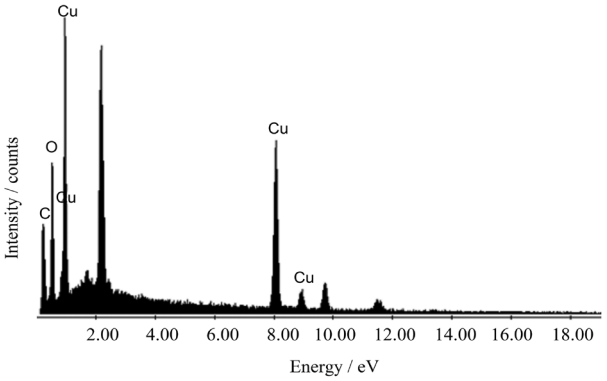

Figure 3. EDS spectrum of the CuO nanofibers.

Electrochemical characterization of CuO-NFs/PIGE

Cyclic voltammetry (CV) was selected to evaluate the electrochemical behavior of CuO-NFs/PIGE. Figure 4 shows the voltammograms recorded in the absence and the presence of glucose at scan rate of 50 mV s^{-1} in 0.1 mol L^{-1} NaOH electrolyte solution. Compared to the background electrolyte response (a), the addition of glucose (b-f) resulted in the increase of the anodic current in the potential range of +0.35 to +0.65 V. The increasing of the glucose concentration causes a proportional enhancement of the oxidative wave. In the reverse scan, no cathodic current was observed as expected for an irreversible oxidation process. Instead, the current of the reverse scan retraces the forward scan in a sigmoidal shape, indicating that the mass transport involves both linear and radial diffusion.

The alkaline medium is necessary to assure the electrocatalytic activity of CuO towards glucose oxidation. According to the literature, the mechanism involves chemisorption of hydroxide ions on the surface of CuO followed by oxidation.[25,26] So, the catalytically active species can be electro-generated via the following reaction (equation 1).

$$CuO + OH^- \rightarrow CuOOH + e^- \quad (1)$$

Regardless of the detailed structure, the redox process can be expressed shortly as Cu^{II}/Cu^{III}. The oxidation of glucose

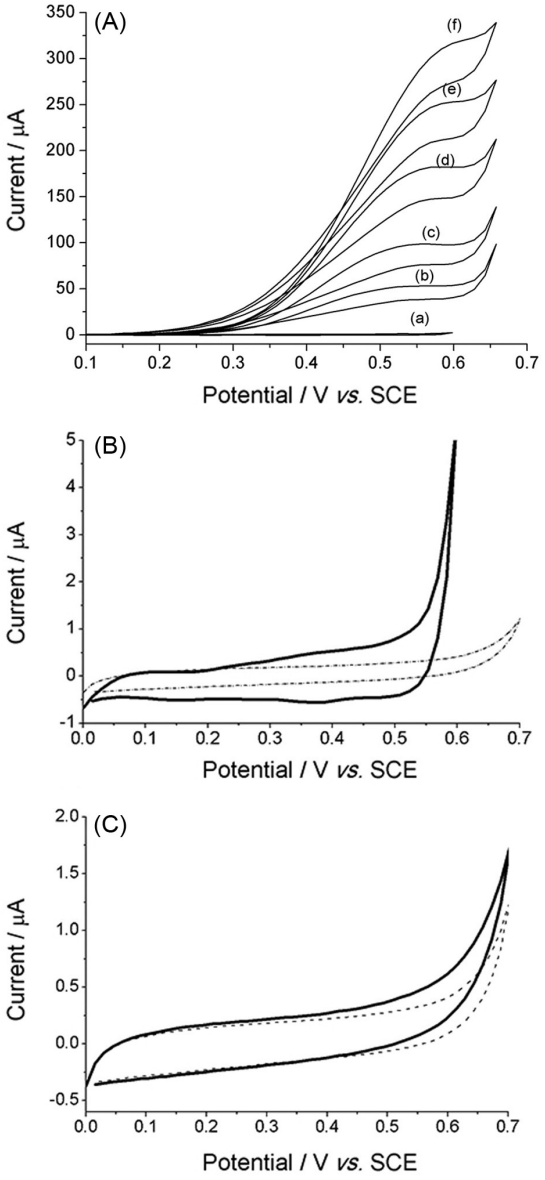

Figure 4. (A) Cyclic voltammograms at CuO-NFs/PIGE in 0.1 mol L^{-1} NaOH solution containing glucose concentrations of 0 (a); 0.5 (b); 1.0 (c); 2.0 (d); 3.0 (e) and 4.0 × 10^{-3} mol L^{-1} (f). (B) CV curves at bare PIGE (dashed line) and CuO-NFs/PIGE (solid line) in 0.1 mol L^{-1} NaOH solution. (C) CV curves at bare PIGE in the absence (dashed line) and presence of 4.0 × 10^{-3} mol L^{-1} of glucose (solid line), in 0.1 mol L^{-1} NaOH solution. Scan rate: 50 mV s^{-1}.

follows a multistep process, where the highly oxidizing Cu^{III} leads to C–C bond cleavage to produce lower molecular weight products.[26] The involvement of CuO nanofibers is confirmed by examining the CVs of unmodified (dashed line) and modified electrodes (solid line) in Figure 4B. It seems that the latter exhibits a shoulder peak attributed to the oxidation of Cu^{II} to Cu^{III} in the same potential range where the whole electrocatalytic process occurs. Furthermore, the appearance of only a small background current at bare PIGE in the presence of glucose (solid line) substantiates the electrocatalytic activity of CuO, see Figure 4C.

The influence of the scan rate (ν) on the glucose oxidation at the CuO-NFs/PIGE is an important parameter about the electrochemical kinetics. Thus, CVs at different scan rates (10-500 mV s^{-1}, data not shown) were recorded in 0.1 mol L^{-1} NaOH containing 1.0 × 10^{-3} mol L^{-1} glucose. The plot of the peak current *versus* the square root of the scan rate reveals a linear relationship which is characteristic of a diffusion-controlled process. The fitting equation is i (mA) = 0.0446 + 0.476 $\nu^{1/2}$ with a correlation coefficient of 0.9983.

Additionally, the electrochemical performance of CuO-NFs/PIGE was evaluated by using $[Fe^{II}(CN)_6]^{3-}$/$[Fe^{III}(CN)_6]^{4-}$ redox system as a probe. Figure 5 depicts the CVs recorded at scan rate ranging from 10 to 1000 mV s^{-1} in 0.1 mol L^{-1} KNO_3 solution containing 1.0 mmol L^{-1} potassium hexacyanoferrate(II).

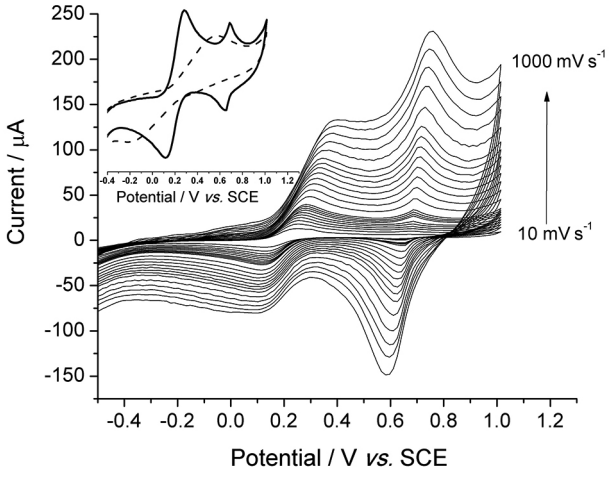

Figure 5. Cyclic voltammograms at CuO-NFs/PIGE in 0.1 mol L^{-1} KNO_3 electrolyte solution containing 1.0 × 10^{-3} mol L^{-1} of $K_4[Fe(CN)_6]$ at different scan rates. Inset: a comparison of the voltammetric behavior between bare PIGE (dashed line) and CuO-NFs/PIGE (solid line) at the scan rate of 200 mV s^{-1}.

Two well-defined oxidation/reduction peaks appeared; the first anodic peak located at +0.40 V and the second at +0.75 V. To get information about the origin of the redox couples the influence of the scan rate on the peak current was analyzed, which reveals different electrochemical behavior. For the first one, the peak current is linearly related to the square root of the scan rate, as depicted in Figure 6a. This response is described mathematically by the Randles-Sevcik equation 2, which predicts the current peak intensity for reversible system under diffusion mass transport control through the expression given bellow.[27]

$$ip = 2.68 \times 10^5 n^{3/2} A D^{1/2} c \nu^{1/2} \quad (2)$$

where ip is the peak current, n is the number of electrons, D is the diffusion coefficient (cm^2 s^{-1}), A is the electrode

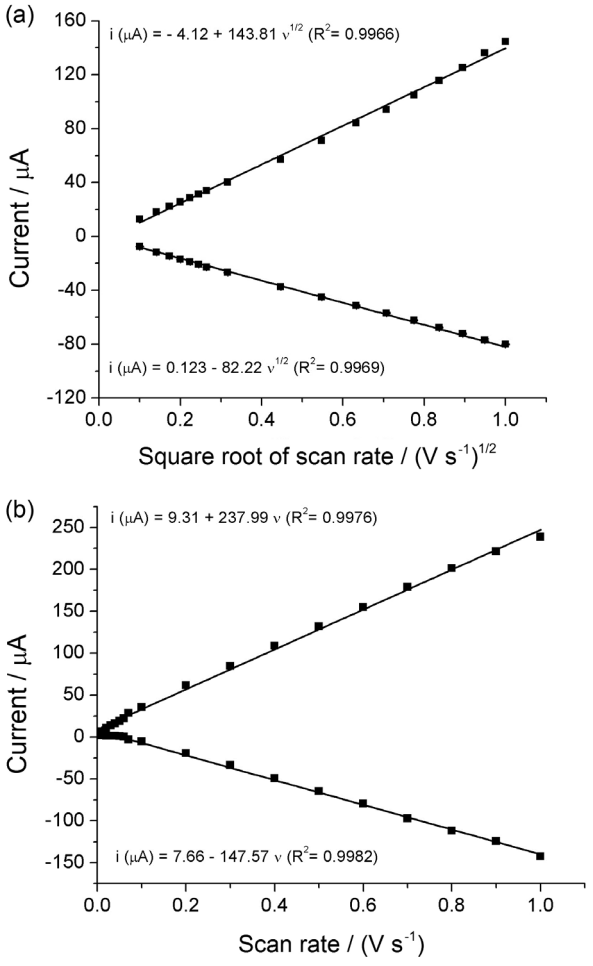

Figure 6. Influence of the potential scan rate on the electrochemical response of $[Fe(CN)_6]^{3-}/[Fe(CN)_6]^{4-}$ at CuO-NFs/PIGE. The dependence of peak current on the square root of the scan rate of the first redox couple (a) and the plot of peak current *versus* the scan rate of the second redox pair (b).

area (cm^2), c is the concentration in mol cm^{-3}, and ν is the potential scan rate (V s^{-1}). This relationship was employed to calculate the active surface area of CuO-NFs/PIGE using the diffusion coefficient of $K_4[Fe(CN)_6]$ reported in the literature.[28] The mean value for three electrodes is 0.19 ± 0.02 cm^2. The diffusion controlled reaction as well as the peak position suggests that the peak located at +0.4 V is attributed to the oxidation of the species present in the solution. On the other hand, the second redox pair exhibits a linear relationship between the peak current and the scan rate (Figure 6b), which is characteristic of a surface controlled electrochemical process. The voltammetric profile is comparable to the reversible process of copper hexacyanoferrate (CuHCF). Accordingly to previous reports, CuHCF exhibits a redox pair at +0.7 V *versus* SCE due to $Cu^{II}[Fe^{II}(CN)_6]^{2-}/Cu^{II}[Fe^{III}(CN)_6]^{-}$.[29,30] The adsorption phenomenon and the peak potential indicate the involvement of the Cu^{II}, therefore, the second redox couple results from the reaction of the species adsorbed on the nanofibers.

Apart from these observations, it is demonstrated that the immobilized CuO significantly improves the electron-transfer behavior. Since a sluggish voltammetric response is observed on the bare PIGE (dashed line) when compared to the CuO-NFs/PIGE (solid line) in the inset of Figure 5. So far, the synthesized CuO nanofibers have demonstrated enhance electron transfer ability, which combined with their large surface area, make them suitable as an electrocatalyst in the glucose oxidation.

Chronoamperometric response of CuO-NFs/PIGE towards glucose oxidation

Chronoamperometry is particularly attractive to carry out electrochemical quantitative analyses. This fixed-potential measurement has the advantages of easy of operation and low background current contribution. The latter allows lowest detection limit. The selection of applied potential becomes relevant to achieve relatively higher current at lower potential value, which at the same time can minimize the electrochemical interference of other species. Accordingly, amperometric current responses were recorded from +0.05 V to +0.625 V in the presence of 1.0 mmol L^{-1} glucose. As shown in Figure 7a, the current response increases with the growth of applied potential until reaching +0.45 V, when almost becomes steady. Thus, a constant potential of +0.45V was selected and employed for the amperometric determination of glucose. This potential is very close to previously reported values for CuO nanofibers,[19,20] but 100 to 200 mV more negative when compare with other CuO nanostructures.[15-17] The decrease in the overpotential suggests that one-dimensional CuO nanofibers significantly enhance the electron transfer reaction of glucose. This improvement may be due to their large surface area or their arrangement in a three-dimensional network.

Figure 7b shows the chronoamperometric curves registered in the concentration range 1.0×10^{-6}-5.6×10^{-3} mol L^{-1} of glucose in 0.1 mol L^{-1} NaOH electrolyte solution. The calibration curve, displayed in the inset of Figure 7, reveals a linear response up to 1.9×10^{-3} mol L^{-1}. The fitting equation is i (μA) = 3.108 + 84.04C (mmol L^{-1}) with a correlation coefficient of 0.9927. The limit of detection was calculated using the equation LOD = 3σ/s, where σ is the standard deviation of the response of 8 blanks, and s is the slope of the calibration curve. The calculated value is 0.39×10^{-6} mol L^{-1}. The sensitivity is 442.1 mA mol^{-1} L cm^2 regarding the calculated active surface area, but becomes 2.7 times higher when considering the

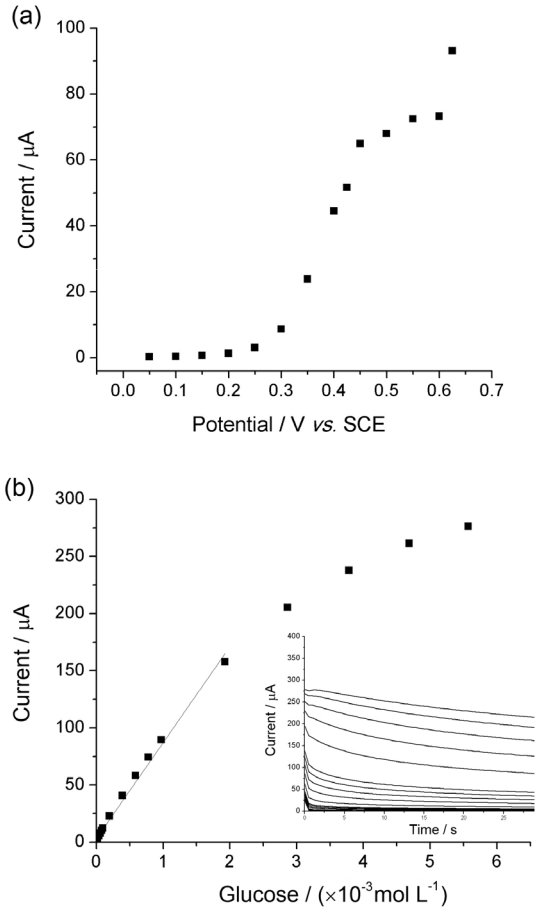

Figure 7. (a) Effect of potential on amperometric response at the CuO-NFs/PIGE in the presence of 1.0×10^{-6} mol L^{-1} glucose, in 0.1 mol L^{-1} NaOH; (b) Chronoamperometric curves obtained at a fixed potential of +0.45 V in the presence of different concentrations of glucose, from 0 to 5.57×10^{-3} mol L^{-1}. The inset presents the corresponding calibration curve.

geometric area of the electrode as in most references. Although the analytical performance of CuO-NFs/PIGE is comparable to other non-enzymatic glucose sensors based on CuO nanostructures,[15,17] it has lower limit of detection than many others as depicted in Table 1.

Stability, reproducibility and interference analysis of the CuO-NFs/PIGE

The reproducibility, stability and selectivity of the sensor were evaluated. The current response of three electrodes gave a relative standard deviation (RSD) of 2.77%, indicating a high reproducibility of the electrode preparation. Shortly 30 seconds of stirring after each determination can prevent electrode fouling from adsorbed oxidation products; ten measurements yielded an RSD of 0.59%. In addition, the stability of CuO-NFs/PIGE was also evaluated by measuring the current during 50 days period. After this time and storing at room temperature in ordinary conditions the electrode retained 90% of its activity, demonstrating its long-term stability.

Since different oxidizable species such as ascorbic acid (AA), uric acid (UA), and dopamine (DA) co-exist with glucose in human serum. The selectivity is a significant factor in the performance of a glucose sensor. Thus, the interference of the above-mentioned species in the response of the CuO-NFs/PIGE was further evaluated. Figure 8 shows the amperometric response towards the addition of 1.0×10^{-3} mol L^{-1} glucose, 0.1×10^{-3} mol L^{-1} of AA, DA, and UA. These concentrations were taken considering that the physiological glucose level is about 30 times higher than the others.[7] Insignificant responses compared to that of glucose can be observed, which indicates a remarkable selectivity of the electrode for glucose detection in the presence of these electroactive molecules. The addition of 0.1×10^{-3} mol L^{-1} of ethanol was also shown not to cause interference.

Real sample analysis

The matrix effect is a recognized problem in quantitative bioanalysis. The applicability and reliability of CuO-NFs/PIGE were tested by calculating the recovery of

Table 1. Comparison of the analytical performance of CuO-NFs/PIGE with other CuO non-enzymatic glucose sensors

Electrode	LOD / (mol L^{-1})	Sensitivity / (mA mol^{-1} L cm^{2})	Linear range / (mol L^{-1})	E / V	Ref.[a]
CuO/nanoflowers/nafion/GCE	1.71×10^{-6}	2,657	10×10^{-6}-5×10^{-3}	0.50 *vs.* Ag/AgCl	13
CuO nanowires/GCE	2.0×10^{-6}	648.2	–	+0.55 *vs.* Ag/AgCl	14
CuO nanoplatelets electrode	0.50×10^{-6}	3,490.7	up to 0.8×10^{-3}	+0.55 *vs.* Ag/AgCl	15
CuO nanorods/graphite	4.0×10^{-6}	371.43	4×10^{-6}-85×10^{-3}	+0.60 *vs.* Ag/AgCl	16
CuO nanospheres/GCE	1.0×10^{-6}	404.53	up to 2.55×10^{-3}	+0.60 *vs.* Ag/AgCl	17
Cu–CuO/C	5.0×10^{-6}	598	up to 3×10^{-3}	+0.75 *vs.* Hg/HgO	18
CuO–NFs/GCE	0.80×10^{-6}	431.3	6×10^{-6}-2.5×10^{-3}	+0.40 *vs.* SCE	19
CuO–NFs/ITO	0.04×10^{-6}	873	0.2×10^{-6}-1.3×10^{-3}	+0.48 *vs.* SCE	20
CuO–NFs/PIGE	0.39×10^{-6}	442.1	1.0×10^{-6}-1.9×10^{-3}	+0.45 *vs.* SCE	This work

[a]Reference; LOD: limit of detection; E: potential; GCE: glassy carbon electrode; C: carbon electrode; ITO: indium tin oxide; PIGE: paraffin-impregnated graphite electrode.

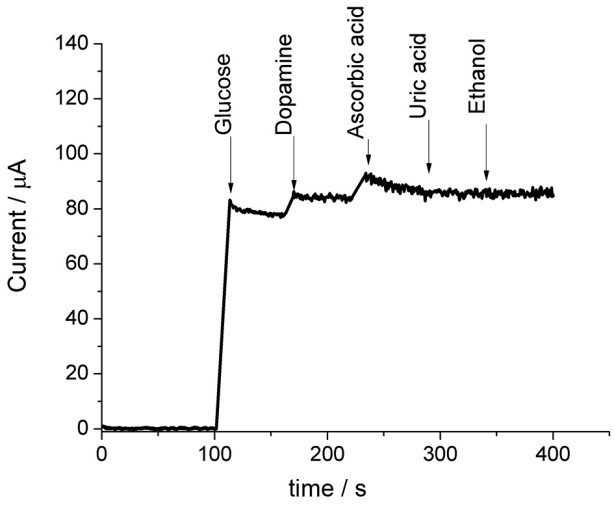

Figure 8. Chronoamperometric responses of CuO-NFs/PIGE with successive additions of 1.0×10^{-3} mol L^{-1} glucose, 0.1×10^{-3} mol L^{-1} DA, 0.1×10^{-3} mol L^{-1} AA, 0.1×10^{-3} mol L^{-1} UA and 0.1×10^{-3} mol L^{-1} ethanol to 1 mol L^{-1} NaOH at +0.45 V.

glucose added to 10.0 mL 0.1 mol L^{-1} NaOH containing 25 μL of blood plasma. The amount of glucose was determined registering the amperometric response at the applied potential of +0.45 V by the standard addition method. Recovery values for glucose in two samples were 99.3 ± 4.5% (n = 3), and 97.5 ± 5.5% (n = 2) indicated a good accuracy of the proposed electrode for the glucose determination.

Conclusions

In summary, CuO nanofibers were successfully synthesized via electrospinning technique. SEM images reveal a three-dimensional network of fibers with large high aspect ratio that can improve the electron transfer reaction. The as-prepared CuO nanofibers were mechanically transferred onto the surface of a paraffin-impregnated graphite electrode. The good electrocatalytic ability, low limit of detection, and easy fabrication make the CuO-NFs/PIGE an excellent electrochemical sensor for glucose detection. In addition, the prepared electrode also showed good reproducibility, stability and selectivity towards common interfering biological species.

Acknowledgements

This research was supported by CNPq (Process: 550441/2012-3) and INCTBio (CNPq/INCT 573672/2008-3). Acknowledgments are also due to Propesq/UFRGS for the financial assistance and the scholarship granted to the first author as part of the Scientific Initiation Program (BIC). The human plasma samples were donated by the Laboratory of Clinical Analysis of the Institute of Cardiology of Rio Grande do Sul, Porto Alegre-RS, Brazil. The authors would like to express their deepest gratitude to Professor Fritz Scholz from Ernst-Moritz-Arndt-Universität Greifswald, Germany for the PIGEs.

References

1. Wild, S.; Roglic, G.; Green, A.; King, H.; *Diabetes Care* **2004**, *27*, 1047.
2. Oliver, N. S.; Toumazou, C.; Cass, A. E. G.; Johnston, D. G.; *Diabetic Med.* **2009**, *26*, 197.
3. Yoo, E. H.; Lee, S. Y.; *Sensors* **2010**, *10*, 4558.
4. Nagaraja, P.; Krishna, H.; Shivakumar, A.; Shrestha, A. K.; *Clin. Biochem*. **2012**, *45*, 139.
5. Wang, J.; *Chem. Rev.* **2008**, *108*, 814.
6. Chen, C.; Xie, Q.; Yang, D.; Xiao, H.; Fu, Y.; Tan, Y.; Yao, S.; *RSC Adv.* **2013**, *3*, 4473.
7. Park, S.; Boo, H.; Chung, T. D.; *Anal. Chim. Acta* **2006**, *556*, 46.
8. Toghill, K. E.; Compton, R. G.; *Int. J. Electrochem. Sci.* **2010**, *5*, 1246.
9. Mu, Y.; Jia, D.; He, Y.; Miao, Y.; Wu, H. L.; *Biosens. Bioelectron.* **2011**, *26*, 2948.
10. Cherevko, S.; Chung, C. H.; *Sens. Actuators, B* **2009**, *142*, 216.
11. Niu, X.; Zhao, H.; Lan, M.; Zhou, L.; *Electrochim. Acta* **2015**, *151*, 326.
12. Zhang, X.; Wang, G.; Liu, X.; Wu, J.; Li, M.; Gu, J.; Liu, H.; Fang, B.; *J. Phys. Chem. C* **2008**, *112*, 16845.
13. Sun, S.; Zhang, X.; Sun, Y.; Yang, S.; Song, X.; Yang, Z.; *Phys. Chem. Chem. Phys*. **2013**, *15*, 10904.
14. Zhang, Y.; Liu, Y.; Su, L.; Zhang, Z.; Huo, D.; Hou, C.; Lei, Y.; *Sens. Actuators, B* **2014**, *191*, 86.
15. Wang, J.; Zhang, W. D.; *Electrochim. Acta* **2011**, *56*, 7510.
16. Wang, X.; Hu, C.; Liu, H.; Du, G.; He, X.; Xi, Y.; *Sens. Actuators, B* **2010**, *144*, 220.
17. Reitz, E.; Jia, W.; Gentile, M.; Wang, Y.; Lei, Y.; *Electroanal.* **2008**, *20,* 2482.
18. Hassan, H. B.; Hamid, Z. A.; *Int. J. Electrochem. Sci.* **2011***, 6*, 5741.
19. Wang, W.; Zhang, L.; Tong, S.; Li, X.; Song, W.; *Biosens. Bioelectron.* **2009**, *25*, 708.
20. Liu, G.; Zheng, B.; Jiang, Y.; Cai, Y.; Du, J.; Yuan, H.; Xiao, D.; *Talanta* **2012**, *101*, 24.
21. Kolmakov, A.; Moskovits, M.; *Annu. Rev. Mater. Res.* **2004**, *34*, 151.
22. Wu, H.; Lin, D.; Pan, W.; *Appl. Phys. Lett.* **2006**, *89*, 133125.
23. Frost, R.; Musumeci, A.; *Spectrochim. Acta A* **2007**, *67*, 48.
24. Gilman, J. W.; VanderHart, D. L.; Kashiwagi, T.; *ACS Symp. Ser*. **1995**, *599*, 161.
25. Xie, Y.; Huber, C. O.; *Anal. Chem.* **1991**, *63*, 1714.

26. Wei, H.; Sun, J. J.; Guo, L.; Li, X.; Chen, G. N.; *Chem. Commun.* **2009**, *20*, 2842.
27. Bard, A. J.; Faulkner, L. R.; *Electrochemical Methods: Fundamentals and Applications*, 2nd ed.; Wiley: New York, 2001.
28. Banks, C. E.; Compton, R. G.; Fisherb, A. C.; Henley, I. E.; *Phys. Chem. Chem. Phys.* **2004**, *6*, 3147.
29. Siperko, L. M.; Kuwana, T.; *Electrochim. Acta* **1987**, *32,* 765.
30. Baioni, A. P.; Vidotti, M.; Fiorito, P. A.; Torresi, S. I. C.; *J. Electroanal. Chem.* **2008**, *622*, 219.

Submitted: March 11, 2015
Published online: June 9, 2015

FAPERGS has sponsored the publication of this article.